

Chaotic mean wind in turbulent thermal convection and long-term correlations in solar activity

A. Bershadskii

*ICAR, P.O.B. 31155, Jerusalem 91000, Israel;
ICTP, Strada Costiera 11, I-34100 Trieste, Italy*

It is shown that correlation function of the mean wind velocity in a turbulent thermal convection (Rayleigh number $Ra \sim 10^{11}$) exhibits exponential decay with a very long correlation time, while corresponding largest Lyapunov exponent is certainly positive. These results together with the reconstructed phase portrait indicate presence of a chaotic component in the examined mean wind. Telegraph approximation is also used to study relative contribution of the chaotic and stochastic components to the mean wind fluctuations and an equilibrium between these components has been studied. Since solar activity is based on the thermal convection processes, it is reasoned that the observed solar activity long-term correlations can be an imprint of the mean wind chaotic properties. In particular, correlation function of the daily sunspots number exhibits exponential decay with a very long correlation time and corresponding largest Lyapunov exponent is certainly positive, also relative contribution of the chaotic and stochastic components follows the same pattern as for the convection mean wind.

PACS numbers: 96.60.Q-, 47.55.pb, 47.52.+j

INTRODUCTION

Turbulent thermal convection is active background for any solar activity. Therefore, the large-scale (coherent) circulations, also known as mean winds, spontaneously generated by turbulent thermal convection must play a significant role in large-scale solar activity. In recent decade a vigorous investigation of statistical properties of the thermal mean winds has been launched [1],[2] (see for a recent review [3]). The winds' dynamics turned out to be very complex and many surprising features were discovered in laboratory experiments and numerical simulations. Simple stochastic models [2],[4] were replaced by more sophisticated stochastic models [3],[6] which also addressed significant three-dimensional nature of the phenomenon. In these models, interaction between the large-scale wind and the small-scale turbulence provides a phenomenological stochastic driving term. Also some deterministic models with chaotic solutions were recently suggested [7],[8], and the idea that a large-scale instability in the developed turbulent convection (caused by a redistribution of the turbulent heat flux) can be an origin of the large-scale coherent structures received certain experimental support (see Ref. [9] and references therein).

It is a difficult problem to distinguish between stochastic and chaotic processes, especially having a developed turbulence as a small-scale background. Observation of the Lorentzian spectra for the mean winds (reported in the Ref. [6]) makes this problem even more difficult. It is shown recently (see, for instance, Ref. [10]) that many properties of the chaotic processes with exponentially decaying correlation function (i.e. with the Lorentzian spectra) can be reproduced by some classical models of stochastic processes (and vice versa). Therefore, for such

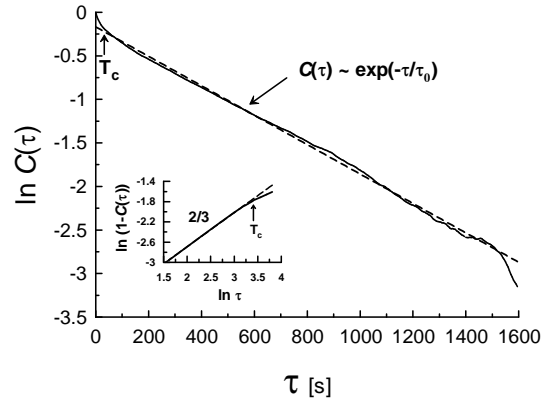


FIG. 1: Autocorrelation function of a mean wind velocity for a Rayleigh-Benard convection laboratory experiment [2],[11]. The dashed straight line indicates the exponential decay Eq. (1). The insert shows a small-time-scales part of the correlation function defect in ln-ln scales. The straight line indicates the Kolmogorov's '2/3' power law for structure function.

chaotic systems stochastic phenomenological models can be rather useful (and relevant). However, it is necessary to reveal an underlying chaotic nature of the phenomenon in order to understand real cause of the long-term correlations in such systems.

CHAOTIC MEAN WIND

Figure 1 shows a correlation function of a mean wind velocity, $v(t)$, measured in a typical thermal convection laboratory experiment in a closed cylindrical container of

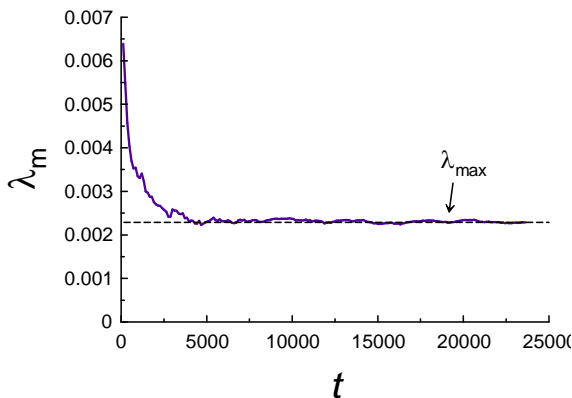


FIG. 2: The pertaining average maximal Lyapunov exponent at the pertaining time, calculated for the same data as those used for calculation of the correlation function (Fig. 1). The dashed straight line indicates convergence to a positive value.

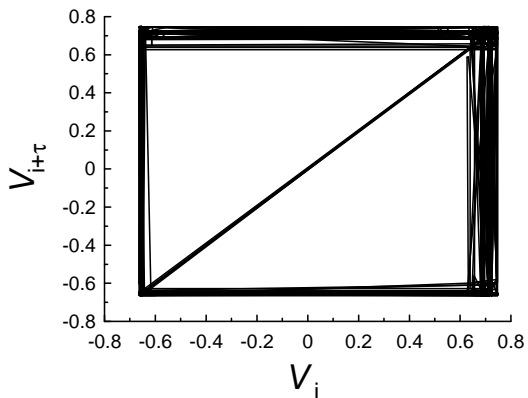


FIG. 3: Phase portrait reconstructed from noise-reduced time series.

aspect ratio 1 for Rayleigh number $Ra \sim 10^{11}$ (see Ref. [2],[11] for description of the experiment and of the other properties of the mean wind). The dashed straight line is drawn in the figure in order to indicate (in the semi-log scales) the exponential decay

$$C(\tau) \sim \exp -(\tau/\tau_0) \quad (1)$$

The correlation time $\tau_0 \simeq 600$ s is very large in comparison with the mean wind circulation period $T_c \simeq 30$ s. The circulation period (turnover time) provides a time scale relevant to the phenomenon physics. The correlation time normalized by this time scale $\tau_0/T_c \sim 20$.

The insert in Fig. 1 shows a small-time-scale part of

the correlation function defect. The ln-ln scales have been used in this figure in order to show a power law (the dashed straight line) for structure function: $\langle (v(t+\tau) - v(t))^2 \rangle$ for $\tau < T_c$:

$$1 - C(\tau) \propto \langle (v(t+\tau) - v(t))^2 \rangle \propto \tau^{2/3} \quad (2)$$

This power law: '2/3', for structure function (by virtue of the Taylor hypothesis transforming the time scaling into the space one [12]) is known for fully developed turbulence as Kolmogorov's power law (cf Refs. [9],[12]).

In order to determine the presence of a deterministic chaos in the time series corresponding to the velocity of the mean wind for the time scales $T_c < t < \tau_0$, we calculated the largest Lyapunov exponent: λ_{max} . A strong indicator for the presence of chaos in the examined time series is condition $\lambda_{max} > 0$. If this is the case, then we have so-called exponential instability. Namely, two arbitrary close trajectories of the system will diverge apart exponentially, that is the hallmark of chaos. At present time there is no theory relating λ_{max} to τ_0^{-1} for chaotic systems. There is only a tentative suggestion that their values should be of the same order. To calculate λ_{max} we used a direct algorithm developed by Wolf et al [13]. Figure 2 shows the pertaining average maximal Lyapunov exponent at the pertaining time, calculated for the same data as those used for calculation of the correlation function (Fig. 1). The largest Lyapunov exponent converges very well to a positive value $\lambda_{max} \simeq 0.0023s^{-1}$.

The ambivalent nature of the turbulence-induced coherent dynamics one can also see in Figure 3. This figure shows a phase portrait reconstructed from the noise-reduced time series for the mean wind velocity.

Thus, we can conclude that the thermal wind under study exhibit chaotic features and the long-term exponential correlation (Fig. 1) is presumably related to this chaotic behavior.

STOCHASTIC-CHAOTIC EQUILIBRIUM

It is shown in Ref. [14] that simple telegraph approximation of stochastic signals can reproduce main statistical properties of these signals. The telegraph approximation of signal $v(t)$ can be constructed as following:

$$u(t) = v(t)/|v(t)| \quad (3)$$

From the definition the telegraph approximation can take only two values: 1 and -1. Figure 4 shows a comparison between correlation function of the full signal for the mean wind velocity $v(t)$ (cf Fig. 1) and correlation function of its telegraph approximation $u(t)$. One can see very good correspondence between these correlation functions. Therefore, certain main statistical properties of the full signal can be studied using the telegraph approximation in this case as well.

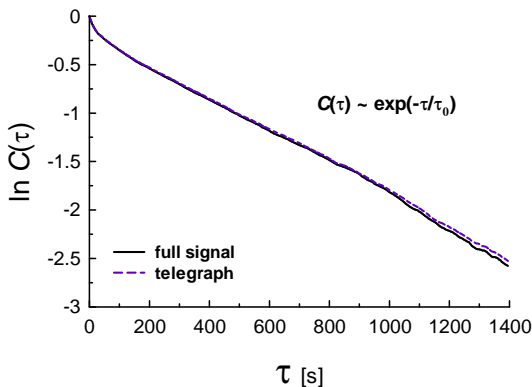


FIG. 4: Autocorrelation functions of a mean wind velocity for a Rayleigh-Benard convection laboratory experiment [2] (solid curve) and of its telegraph approximation (dashed curve).

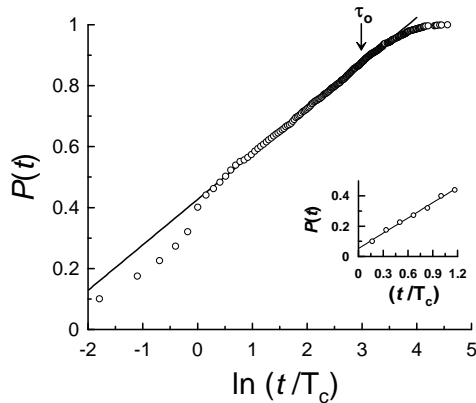


FIG. 5: Cumulative probability $P(t)$ (Eq. (5)) vs. $\ln(t/T_c)$. The straight line indicates correspondence to Eq. (6). The insert shows a linear dependence of $P(t)$ on t/T_c for $t \leq T_c$.

Very significant characteristic of the telegraph signal is duration, τ , of the continuous intervals (boxes) where the signal takes value 1 or value -1. Probability density function of the duration (or life) times τ : $p(\tau)$, for the telegraph approximation of the mean wind velocity signal was studied in detail in Ref. [2]. It has a peak at $\tau \simeq T_c$. In the the range $T_c < \tau < \tau_0$ the probability density exhibits a power law

$$p(\tau) \simeq c \tau^\alpha \quad (4)$$

with the value of the exponent α close to -1 . For $\tau > \tau_0$ the probability density $p(\tau)$ decays exponentially, as it should be for the random telegraph signal. Figure 5

shows cumulative probability

$$P(t) = \int_0^t p(\tau) d\tau \quad (5)$$

In the semi-logarithmical scales the straight line indicates just the power law for $p(\tau)$ (Eq. (4) with $\alpha \simeq -1$):

$$P(t) \approx P(T_c) + c \int_{T_c}^t \tau^{-1} d\tau \approx P(T_c) + c \ln(t/T_c) \quad (6)$$

where $P(T_c)$ is a constant part provided by the turbulent component to the cumulative probability $P(t)$ for $\tau_0 > t > T_c$. On the whole,

$$P(\infty) \simeq \Delta P + c \ln(\tau_0/T_c) \quad (8)$$

where

$$\Delta P = P(T_c) + \int_{T_c}^{\infty} p(\tau) d\tau \quad (9)$$

i.e. ΔP is contribution of the *stochastic* components: turbulence and the large-scale random telegraph signal, to the total cumulative probability. In our case there is a probabilistic equipartition of the stochastic and chaotic components to the total cumulative probability $P(\infty) = 1$: $\Delta P \simeq 0.5 \pm 0.04$. If this probabilistic equipartition is universal and the constant c in the power law Eq. (4) is also universal (at least asymptotically), then

$$\ln(\tau_0/T_c) = \frac{1 - \Delta P}{c} \approx 0.5/c \quad (10)$$

is universal as well. From the present data we can estimate: $c \approx 0.16 \pm 0.01$, and $\ln(\tau_0/T_c) \approx 3$ (see also below).

This kind of probabilistic equipartition is usually related to statistical restoration of a symmetry. For instance, the spontaneous appearing of the mean wind results in a spontaneous breaking of mirror (or parity - P) symmetry. Statistical restoration of the parity (P-symmetry) means probabilistic equipartition of the $u(t) = 1$ and $u(t) = -1$ events (Eq. (3)). This probabilistic equipartition indeed takes place in present case and it is clear evidence of the statistical restoration of the P-symmetry (the directions of the mean wind rotation: clockwise and anticlockwise, are statistically equivalent). While the P-symmetry arises from space inversion, the T-symmetry arises from time reversal (reversibility). In the present case both P- and T-transformations result in the same mean wind switching: $u \rightarrow -u$. It can be just statistical restoration of the combined PT-symmetry (statistical invariance under joint action of parity and time reversal) that results in the equal probability of the reversible (chaotic) and irreversible (random) switchings. The statistical restoration of the symmetry in a mixed stochastic-chaotic motion indicates an equilibrium reached between the stochastic and chaotic components (SC-equilibrium).

For the closed orbits in the chaotic systems the Bowen's theorem [15] is an analogue of ergodic theorem. This theorem provides a basis for the equality of the average over the phase space and the average over large-period orbits. Let us now, in the terms of the Bowen's theorem (cf. also [16]), consider a phase volume subregion $\Delta\Omega$: $\Omega_c < \Delta\Omega \ll \Omega$ (where Ω_c is phase volume corresponding to the upper turbulent scale T_c) and all the periodic trajectories passing through it. Different closed orbits can be distinguished by their period T . Their distribution does not depend significantly on location and boundaries of the subregion $\Delta\Omega$. Moreover, if we consider the periodic orbits with periods in the interval $(T, T+t)$ passing through the region, then we can use an estimate

$$\frac{t}{T_c} \approx \frac{\Delta\Omega}{\Omega_c} \quad (11)$$

(the coarse graining is defined by the partition of phase space by the cells Ω_c). Let us consider an entropy corresponding to the subregion $\Delta\Omega$ (cf. Ref. [16]) and use estimate Eq. (11)

$$S = \beta \ln \frac{\Delta\Omega}{\Omega_c} \approx \beta \ln \frac{t}{T_c} \quad (12)$$

where β is a constant (see below, and cf. also Ref. [17] for quantum chaos). The logarithmic growth of entropy can imply certain self-similarity of joint probabilistic properties of the time series $v(t) \leftrightarrow u(t)$ (see Eq. (3)). Indeed, let us consider probability distribution function, $p(v, t)$, for the signal v at the impulses (boxes) of length $\tau \leq t$ of its telegraph approximation u . For the stationary signal the self-similarity has a standard form [18]

$$p(v, t) = \frac{1}{t^\beta} f\left(\frac{v}{t^\beta}\right) \quad (13)$$

where f is certain function of the argument v/t^β (the statistical restoration of the parity has been taken into account here). Let us consider an entropy

$$S(t) = - \int dv p(v, t) \ln p(v, t) \quad (14)$$

Changing the integration variable: $v \rightarrow v/t^\beta$ and using equilibrium condition: $S(T_c) = 0$, one obtains from Eqs. (13) and (14):

$$S(t) = \beta \ln(t/T_c) \quad (15)$$

(cf Eq. (12)).

The insert in Fig. 5 shows a linear dependence of $P(t)$ on t/T_c for the turbulent regime that can be related to an analytic dependence of $P(t)$ on t/T_c for $0 < t/T_c \leq 1$ (the linear dependence represents the first two terms approximation of the Taylor expansion; the small 'jump' at the point $t = 0$ is presumably related to transition from laminar to turbulent motion). In a vicinity of the

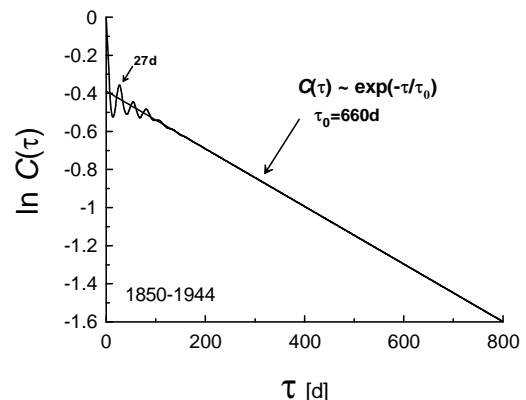


FIG. 6: Autocorrelation function of the daily sunspots number for period 1850-1944y.

SC-equilibrium $P(t)$ is an analytic function of the entropy $S(t) = \beta \ln(t/T_c)$. Applying again the Taylor expansion we obtain

$$P(t) = P(T_c) + c_o S(t) + \dots \approx P(T_c) + c_o \beta \ln(t/T_c) \quad (16)$$

where $c_o = (\partial P / \partial S)|_{S=0}$ (cf. Fig. 5 and Refs. [16],[19] for the transformation $t \rightarrow \ln t$).

It is possible that the above consideration is also applicable for the large-scale coherent structures observed in other turbulent flows (in turbulent boundary layers, for instance [20]). If, for instance, at the SC-equilibrium the exponent β is a global invariant of motion and its value is the same for $t < T_c$ and for $t > T_c$, then, taking into account that the dimensionless entropy $S(\tau_0) = 1$ one obtains from Eq. (15): $\ln(\tau_0/T_c) = 1/\beta$. For the Brownian processes $\beta = 1/2$, whereas for the Kolmogorov's scaling: Eq. (2), one has $\beta = 1/3$. For Kolmogorov's turbulence as a background it results in estimate: $\ln(\tau_0/T_c) = 3$ (cf. above). If the background turbulence produces scaling different from the Kolmogorov's one, then value of the β -exponent can be different from $1/3$. For the Kraichnan's scaling, for instance [21], $\beta = 1/4$ and, consequently, $\ln(\tau_0/T_c) = 4$ (i.e. in the case of the Kraichnan's background turbulence the correlations related to the large-scale coherent structures are even more long-term than those generated by the Kolmogorov's background turbulence).

CHAOTIC SOLAR ACTIVITY

Let us now look at solar activity, which usually measured in the sunspots number (SSN). In the Babcock-Leighton scenario [22]-[25], for instance, the surface generated poloidal magnetic field is carried to the bottom

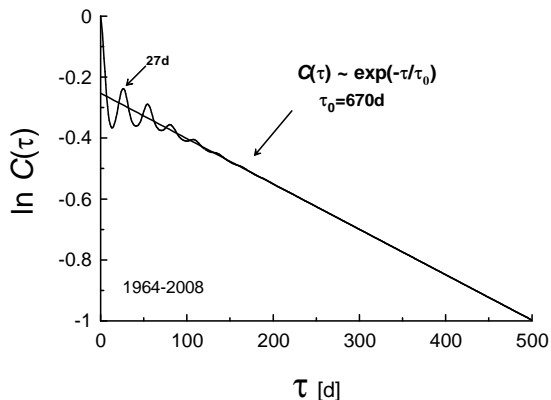


FIG. 7: Autocorrelation function of the daily sunspots number for period 1964-2008y.

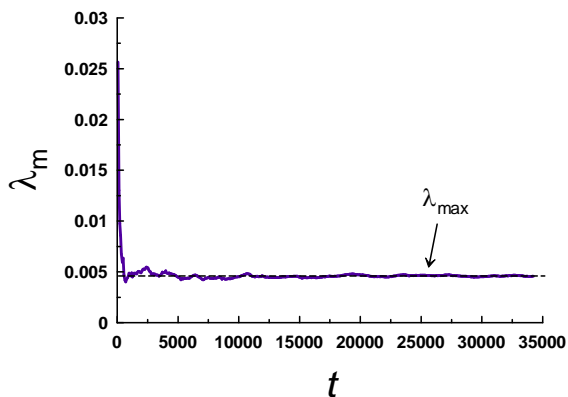


FIG. 8: The pertaining average maximal Lyapunov exponent at the pertaining time, calculated for the same data as those used for calculation of the correlation function shown in Fig. 6. The dashed straight line indicates convergence to a positive value.

of the *convection* zone by turbulent diffusion or by the meridional circulation. The toroidal magnetic field is produced from this poloidal field by differential rotation in the bottom shear layer. Destabilization and emergence of the toroidal fields (in the form of curved tubes) due to magnetic buoyancy can be considered as a source of pairs of sunspots of opposite polarity. The turbulent thermal convection in the convection zone captures the magnetic flux tubes and either *disperses* or *pulls* them through the surface to become sunspots. This means, that the chaotic mean winds of the thermal convection should play a significant role in generation and transportation of the magnetic field, and consequently in the solar activ-

ity. Therefore, the chaotic nature of these winds should imprint itself in the statistical properties of the solar activity. In particular, the long-term correlation present in these winds should result in a long-term correlation in the solar activity. Indeed, Figure 6 shows correlation function of the daily sunspots number (SSN) for period 1850-1944y (the SSN data were taken from [26]). Next to this period two 11-year solar cycles were extraordinary active (see, for instance, Ref. [27]) and, therefore, we excluded them from the consideration. For the last four solar cycles (period 1964-2008y) solar activity was again stable (though rather strong) and in figure 7 we show the daily SSN correlation function for this period. The semi-log scales were used in the Figs. 6 and 7 in order to exhibit exponential decay, which corresponds to straight line in these scales. It should be noted that the maximum entropy method was used in these calculations, because it provides an optimal resolution even for relatively small data sets. The oscillations in these figures correspond to the solar rotation period $\simeq 27$ days. This period roughly corresponds to rotation at a latitude of 26° , which is consistent with the typical latitude of sunspots. The apparent straight lines correspond to the exponential decay Eq. (1) (cf Fig. 1). The decay rate (or correlation time) takes very close values for these two time periods: $\tau_0 \simeq 660$ d for the period 1850-1944y and $\tau_0 \simeq 670$ d for the period 1964-2008y. This correlation time is considerably larger than the circulation periods inside the convection zone T_c , which are of order of the solar rotation period. It should be noted that the correlation time normalized with the circulation time is close to the normalized correlation time of the thermal mean wind $\ln(\tau_0/T_c) \sim 3$ (cf previous section). Taking into account previous consideration one can assume that this long-term correlation in the solar activity could be related to the chaotic mean winds in the turbulent solar thermal convection. In order to support this assumption we show in figure 8 the pertaining average maximal Lyapunov exponent calculated for the daily SSN data for the period 1850-1944y. The largest Lyapunov exponent converges very well to a positive value $\lambda_{max} \simeq 0.0047d^{-1}$, indicating chaotic nature of the long-term correlations in the solar activity.

DISCUSSION

Most of known chaotic systems exhibit exponentially decaying correlation functions (see, for instance, Refs. [10],[28]) or exponentially decaying spectral functions (see, for instance, [29],[30]). It is shown in a recent paper Ref. [31] that solar activity at *decadal* time scales exhibit chaotic behavior of the second kind (see for a possible underlying physical mechanism Ref. [32]). In present paper we have provided certain evidences that at *daily* (to annual) time scales the solar activity

exhibits a chaotic behavior of the first kind. In this case the underlying physical mechanism can be related to chaotic nature of the mean (coherent) winds spontaneously generated by turbulent thermal convection. The observed long-term exponentially decaying correlation functions and the positive largest Lyapunov exponents for both: mean wind and solar activity, situations can be considered as an argument for this suggestion. One should also take into account, that the turbulent thermal convection plays crucial role in solar activity. Therefore, the large-scale (coherent) processes generic to the turbulent thermal convection must imprint their statistical properties on the solar activity by one way or another.

The author is grateful to J.J. Niemela, to K.R. Sreenivasan, and to the SIDC-team, the World Data Center for the Sunspot Index, the Royal Observatory of Belgium for sharing their data and discussions.

-
- [1] L.P. Kadanoff, *Phys. Today* **54**, 34 (2001).
- [2] K.R. Sreenivasan, A. Bershadskii, and J. Niemela, *Phys. Rev. E* **65**, 056306 (2002).
- [3] A. Ahlers, S. Grossmann, and D. Lohse, *Rev. Mod. Phys.*, **81**, 503 (2009).
- [4] R. Benzi, *Phys. Rev. Lett.*, **95**, 024502 (2005).
- [5] R. Benzi and R. Verzicco, *Europhys. Lett. (EPL)*, **81**, 64008 (2008).
- [6] E. Brown, and G. Ahlers, *Phys. Fluids* **20**, 075101 (2008).
- [7] A.F Fontenele, S. Grossmann, and D. Lohse, *Phys. Rev. Lett.* **95**, 084502 (2005).
- [8] C.R. Resagk et al., *Phys. Fluids* **18**, 095105 (2006).
- [9] M. Bukai, A. Eidelman, T. Elperin, et al., *Phys. Rev. E*, **79**, 066302 (2009).
- [10] V.S. Anishchenko et al., *Physica A*, **325** 199 (2003).
- [11] J. Niemela, L. Skrbek, K. R. Sreenivasan, and R. J. Donnelly, *J. Fluid Mech.* **449**, 169 (2001).
- [12] A. S. Monin and A. M. Yaglom, *Statistical Fluid Mechanics, Vol. II* (MIT Press, Cambridge, 1975).
- [13] A. Wolf, J.B. Swift, H.L. Swinney, and J.A. Vastano, *Physica D*, **16**, 285 (1985).
- [14] K.R. Sreenivasan and A. Bershadskii, *J. Stat. Phys.*, **125**, 1141 (2006).
- [15] R.Z. Sagdeev, D.A. Usikov, G.M. Zaslavsky, *Nonlinear physics. From the pendulum to turbulence and chaos*, (Harwood Academic Publishers, NY, 1988).
- [16] V. Afraimovich, and G.M. Zaslavsky, *Chaos*, **13**, 519 (2003).
- [17] I. Guarneri, *Annales de l'Institut H.Poincare*, **68** 491 (1998).
- [18] G.I. Barenblatt, *Similarity, Self-similarity and Intermediate Asymptotics* (Consultants Bureau, New York, 1979).
- [19] W.G. Hoover, *Phys. Rev., A*, **37**, 252, (1988).
- [20] K.R. Sreenivasan, private communication.
- [21] J. Cho, A. Lazarian, and E. Vishniac, *Lect. Notes Phys.*, **614**, 56 (2003).
- [22] H.W. Babcock, The topology of the suns magnetic field and the 22-year cycle, *ApJ*, **133**, 572 (1961).
- [23] R.B. Leighton, A Magneto-Kinematic Model of the Solar Cycle, *ApJ*, **156**, 1 (1969).
- [24] M. Dikpati, G. de Toma, and P.A. Gilman, Predicting the strength of solar cycle 24 using a flux-transport dynamo based tool, *Geophys. Res. Lett.*, **33** L05102 (2006).
- [25] A.R. Choudhuri, P. Chatterjee, and J. Jiang, Predicting Solar Cycle 24 With a Solar Dynamo Model, *Phys. Rev. Lett.* **98**, 131101 (2007).
- [26] Available at <http://sidc.oma.be/sunspot-data/>.
- [27] I.G. Usoskin, S.K. Solanki, M. Schüssler, et al., Millennium-Scale Sunspot Number Reconstruction: Evidence for an Unusually Active Sun since the 1940s, *Phys. Rev. Lett.* **91**, 211101 (2003).
- [28] D. Ruelle, Resonances of chaotic dynamical systems, *Phys. Rev. Lett.*, **56**, 405 (1986).
- [29] D.E. Sigeti, Survival of deterministic dynamics in the presence of noise and the exponential decay of power spectrum at high frequencies. *Phys. Rev. E*, **52**, 2443 (1995).
- [30] N. Ohtomo, K. Tokiwano, Y. Tanaka, et al, Exponential Characteristics of Power Spectral Densities Caused by Chaotic Phenomena, *J. Phys. Soc. Jpn.*, **64** 1104 (1995).
- [31] A. Bershadskii, Transitional dynamics of the solar convection zone, *EPL (Europhys. Lett.)*, **85**, 49002 (2009).
- [32] J. Feynman, and S.B. Gabriel, Period and phase of the 88-year solar cycle and the Maunder Minimum: Evidence for a chaotic Sun, *Solar Physics*, **127**, 393 (1990).